

Electronic Supplementary Information

A facile route to diverse assemblies by host-guest recognition

Xing Zhou^{1,2,†}, Songling Han^{1,†}, Qixiong Zhang¹, Yin Dou^{1,2}, Jiawei Guo¹, Ling Che^{1,3}, Xiaohui Li^{2,}, Jianxiang Zhang^{1,*}*

¹ Department of Pharmaceutics, College of Pharmacy, Third Military Medical University, Chongqing 400038, China

² Institute of Materia Medica, Third Military Medical University, Chongqing 400038, China

³ Department of Pharmacy, Hospital 309 of PLA, Beijing 100091, China

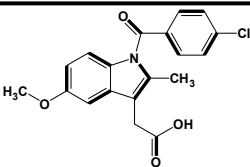
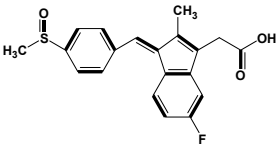
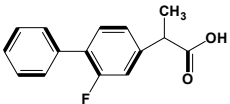
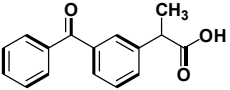
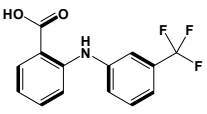
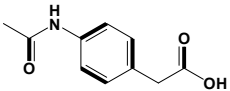
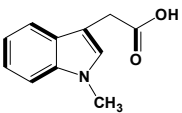
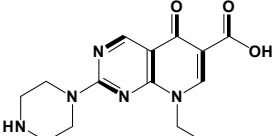
[†]These authors contributed equally to this study.

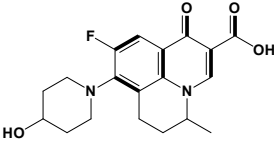
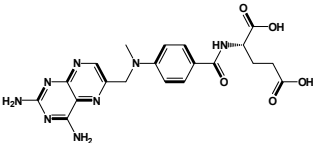
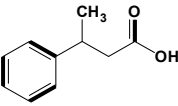
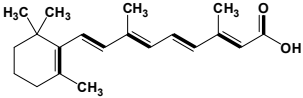
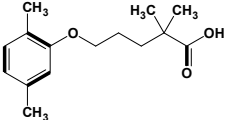
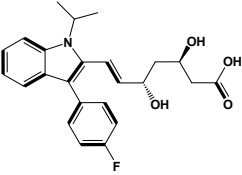
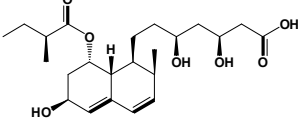
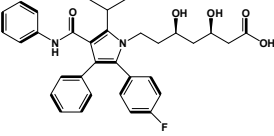
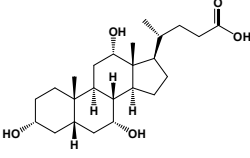
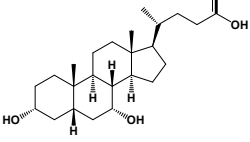
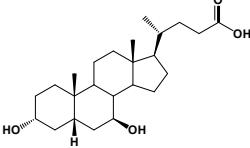
Correspondence should be addressed to J.X.Z (jxzhang@tmmu.edu.cn; jxzhang1980@gmail.com) and X.H.L (lpsh008@aliyun.com)

Table S1 Molecular weight (Mw) of various polymers.

Polymers	Mw (kDa)
PAm	10
PNMAm	26
PNEAm	23
PNPAm	18
PHEAm	23
PNBAm	14
PNTBAm	11
PNHAm	13
PDMAm	20
PDEAm	19

Table S2 Various carboxyl bearing compounds (CBCs) involved in this study.

Compounds	Abbreviation	Formula	Activity
Indomethacin	IND		A NSAID used to treat osteoarthritis, rheumatoid arthritis, and ankylosing spondylitis.
Sulindac	SUL		A NSAID used to treat acute and chronic inflammatory conditions.
Flurbiprofen	FLUR		A NSAID used to treat inflammation and pain of arthritis.
Ketoprofen	KET		A NSAID with analgesic and antipyretic effects.
Flufenamic acid	FLA		A drug with analgesic, anti-inflammatory, and antipyretic properties, as well as an ion channel modulator.
<i>p</i> -Acetamidophenyl acetic acid	APA		An anti-inflammatory drug used to treat rheumatoid arthritis.
1-Methyl-3-indoleacetic acid	MIAA		An anti-inflammatory compound.
Pipemidic acid	PIP		A drug with bactericidal activity by inhibiting DNA gyrase.

Nadifloxacin	NAD		An antibiotic for the treatment of acne vulgaris and bacterial skin infections.
Methotrexate	MET		An antimetabolite drug used to treat cancer and autoimmune diseases.
4-Phenylbutyric acid	PBA		A chemical chaperone that can alleviate endoplasmic reticulum stress, regulate cell death and autophagy as well as treat atherosclerosis.
Retinoic acid	RA		A drug used to treat cancer, cardiac remodeling, and coronary artery disease.
Gemfibrozil	GEM		A drug used to treat cardiovascular diseases such as hyperlipidemia and hypertriglyceridemia.
Fluvastatin	FLS		A drug used to treat hypercholesterolemia and prevent cardiovascular disease.
Pravastatin	PRAS		A drug used to treat dyslipidemia and prevent cardiovascular disease.
Atorvastatin	ATS		A drug used to treat dyslipidemia and prevent cardiovascular disease.
Cholic acid	CA		A bile acid.
Chenodeoxycholic acid	CDCA		A compound used to treat hepatitis C infection and cerebrotendinous xanthomatosis.
Hyodeoxycholic acid	HDCA		A natural compound that can treat increased plasma cholesterol levels and atherosclerosis as well as prevent cholesterol-induced gallstones.

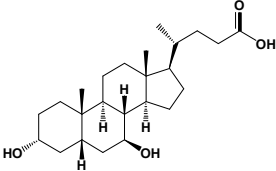
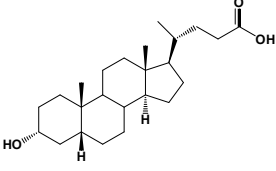
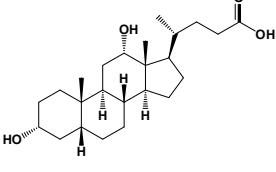
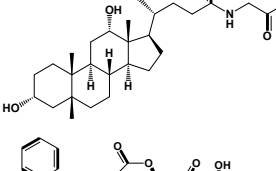
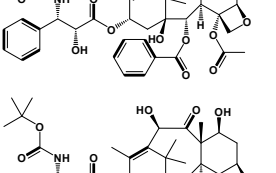
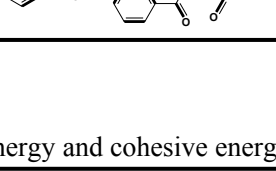
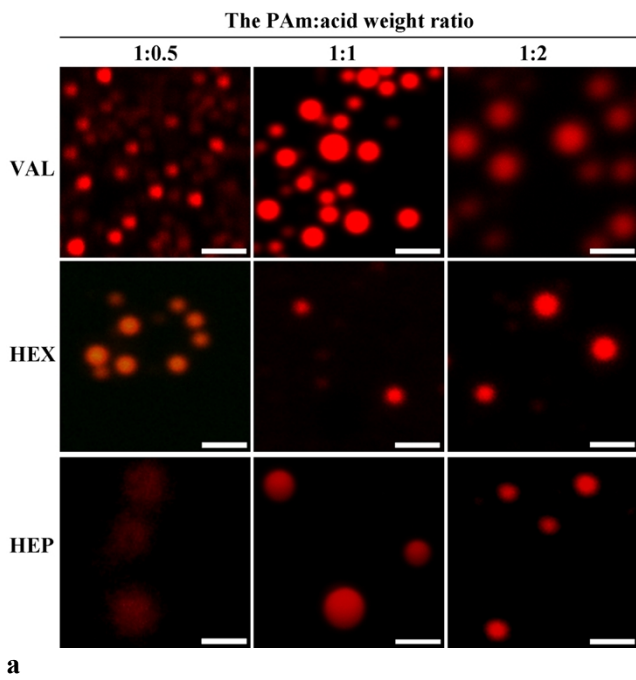
Ursodeoxycholic acid	UDCA		A FDA approved drug used to treat gallstones and primary biliary cirrhosis.
Lithocholic acid	LCA		A natural compound that can selectively kill neuroblastoma cells.
Deoxycholic acid	DOCA		A bile acid used to prevent and dissolve gallstones, employed in mesotherapy injections, and also used as an immunostimulant.
Glycodeoxycholic acid	GDCA		A bile acid derived from deoxycholic acid and glycine.
Paclitaxel	PTX		A mitotic inhibitor and antiproliferative agent for the treatment of cancer and restenosis.
Docetaxel	DTX		An antimitotic drug for cancer therapy.

Table S3 The calculated values of cohesive energy and cohesive energy density of typical CBCs.

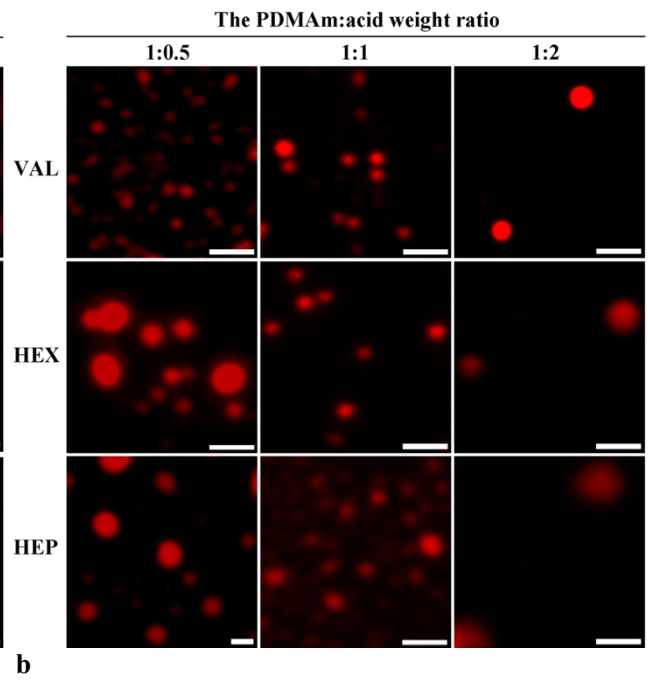
Compounds	Cohesive energy (CE) (cal/mol)	Cohesive energy density (CED) (cal/cm ³)
VAL	11265	102.1
HEX	12445	98.5
HEP	13625	95.6
IND	36158	172.3

Table S4 Estimated binding energy values using different searching algorithms built in AutoDock 4.2.

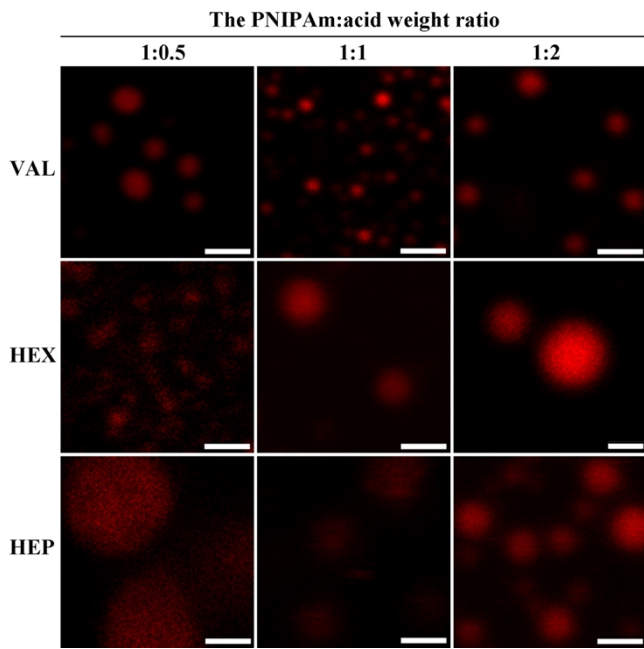
Algorithms	Estimated binding energy (kcal/mol)		
	PAm	PDMAm	PNIPAm
GA	-1.8	-2.2	-3.2
LGA	-2.0	-2.7	-4.0
LS	-1.5	-1.7	-2.8
SA	-1.0	-0.9	-2.1



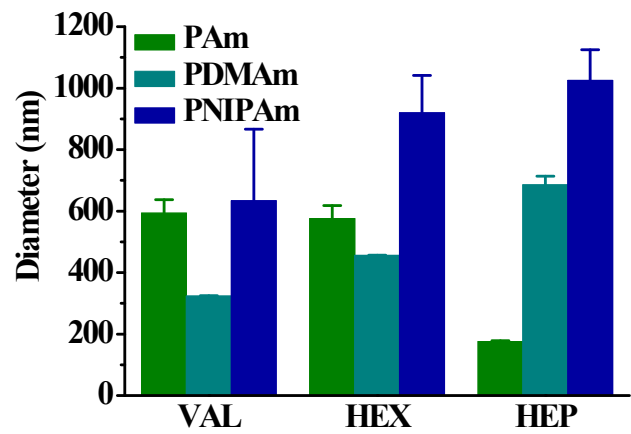
a



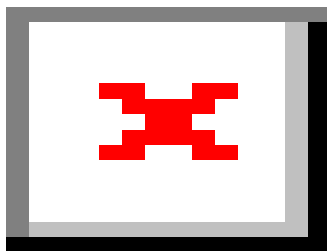
b



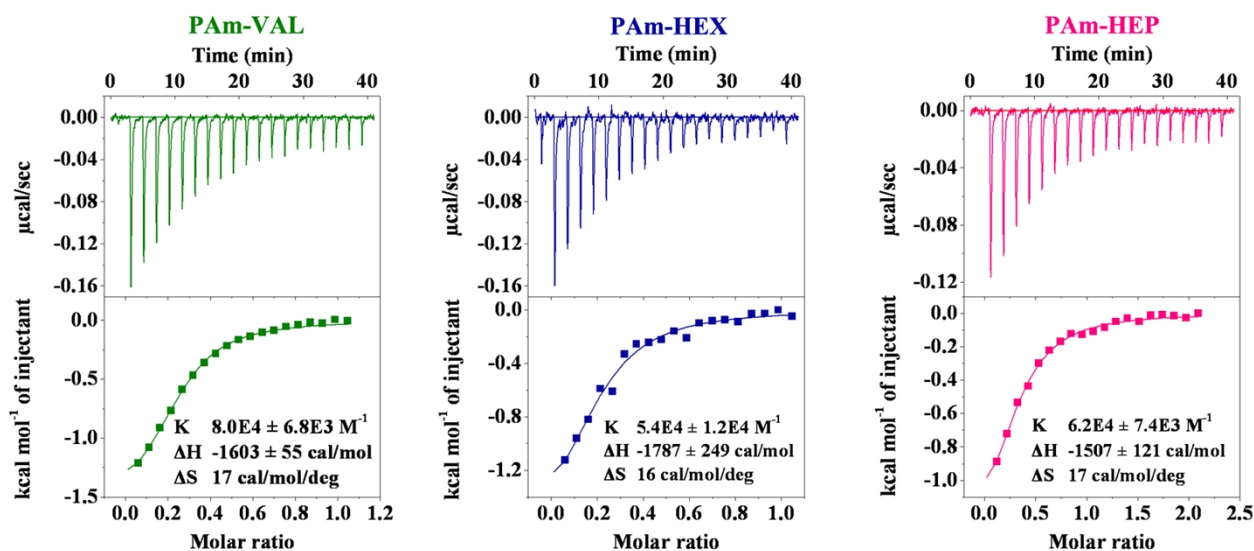
c



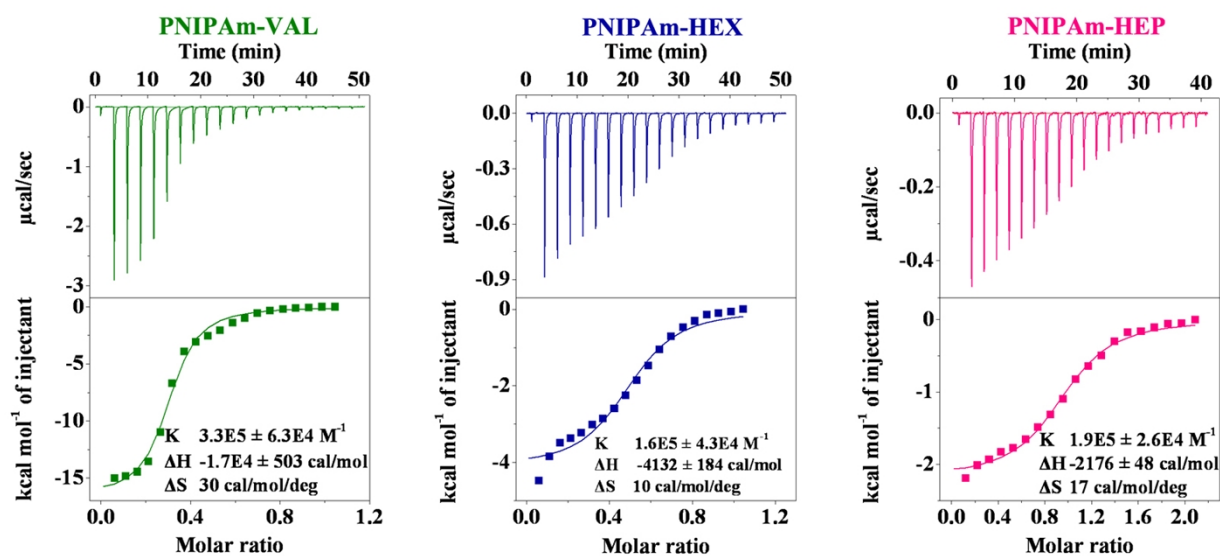
d



e



f



g

Fig. S1 Assembly of PAm, PDMAm, and PNIPAm with typical aliphatic acids of valeric acid (VAL), hexanoic acid (HEX), and heptanoic acid (HEP). Trace amount of Nile red was used to label assemblies. **a-c**, CLSM images of assemblies based on PAm (a), PDMAm (b), and PNIPAm (c) with various acids at the polymer/acid weight ratio of 1:0.5, 1:1, or 1:2. The scale bars represent 1 μ m. **d**, Mean size of microparticles assembled at the polymer/acid weight ratio of 1:1. **e**, TEM images of assemblies derived from VAL or HEX with different polymers. **f-g**, ITC profiles of PAm (f) or PNIPAm (g) and various aliphatic acids in aqueous solution. PNIPAm with Mw of 2 kDa was employed.

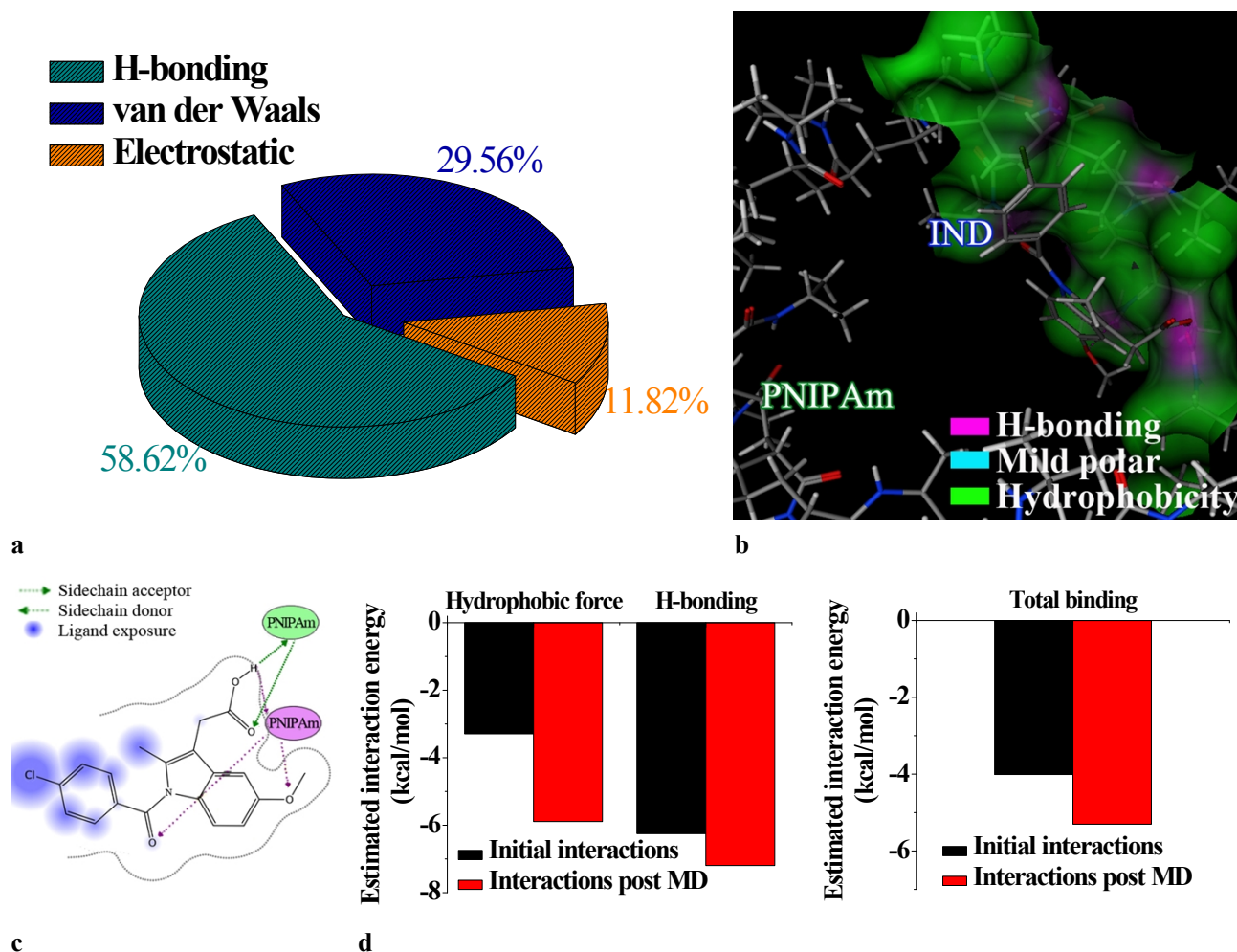
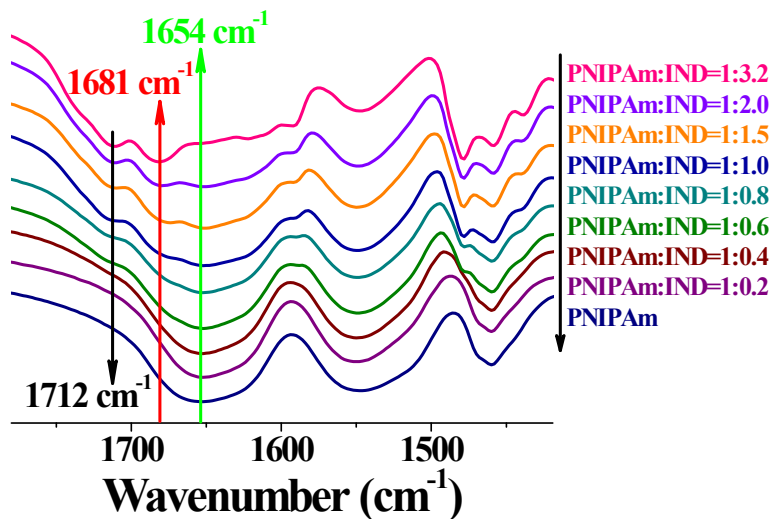
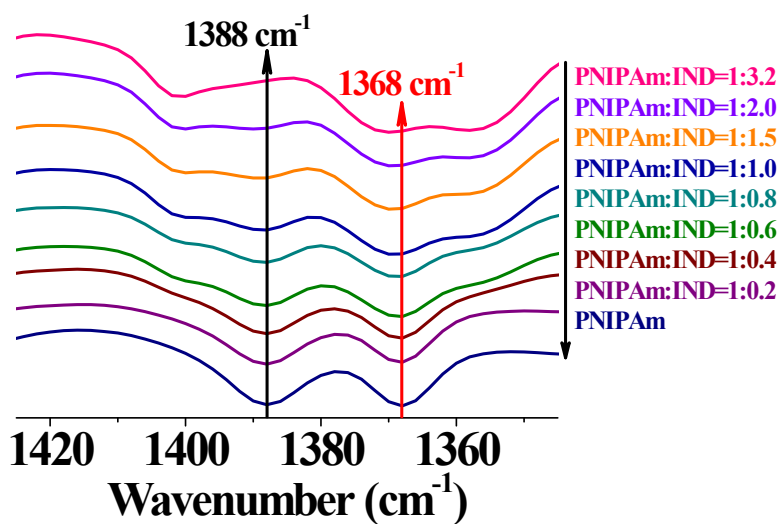


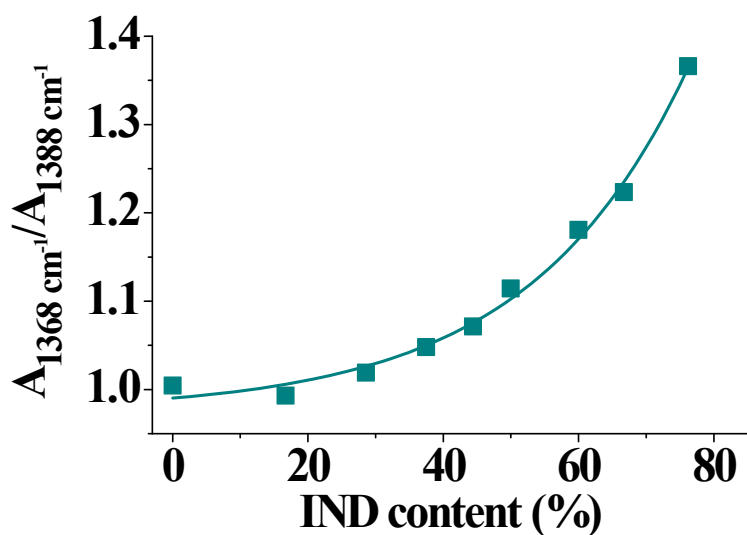
Fig. S2 Computational simulation of interactions between IND and PNIPAm after the MD process. **a**, The relative contribution of various forces to the total binding free energy in the IND/PNIPAm system. **b**, The 3D conformation of IND/PNIPAm after MD at 1:1 in water. **c**, The 2D profile showing interactions between IND and PNIPAm before (green) and after (purple) MD at the PNIPAm/IND molar ratio of 1:1. **d**, The estimated intermolecular energy and binding energy of IND/PNIPAm before and after the MD process. The hydrophobic forces were contributed by the C-C hydrophobic effect. H-bonding and total binding mean the related free energy estimated by AutoDock 4.2.



a



b



c

Fig. S3 IND/PNIPAm interactions characterized by FT-IR spectroscopy. **a-b**, Locally magnified FT-IR spectra illustrating bands related to carbonyl in IND and PNIPAm (a) as well as absorbance associated with isopropyl (b). **c**, Changes in the absorbance ratio of isopropyl vibration bands at 1368 ($A_{1368 \text{ cm}^{-1}}$) and 1388 cm^{-1} ($A_{1388 \text{ cm}^{-1}}$) as a function of the IND content. PNIPAm with Mw of 10 kDa was used.

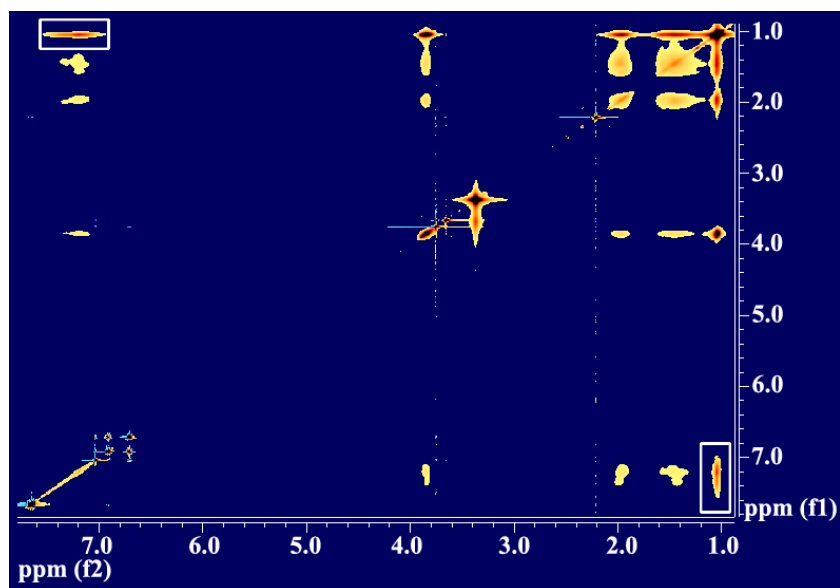
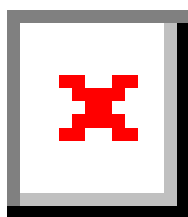
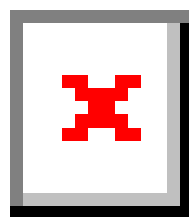


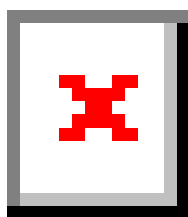
Fig. S4 The ^1H - ^1H 2D Noesy spectrum of IND/PNIPAm in DMSO-d_6 . The white rectangles indicate the correlation signals. The weight ratio of IND/PNIPAm was 1:1. PNIPAm with Mw of 10 kDa was used.



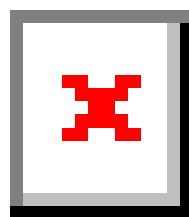
a



b

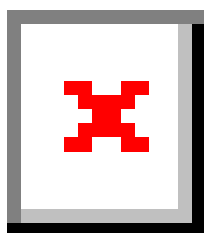


c

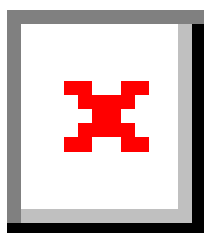


d

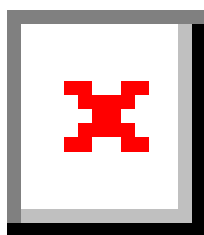
Fig. S5 The effect of processing temperature on assembly of IND/PNIPAm. **a-b**, SEM (a) and TEM (b) images of samples dialyzed at 4°C . **c-d**, SEM (c) and TEM (d) micrographs of samples obtained at 50°C . PNIPAm with Mw of 10 kDa was used. When assembly of IND/PNIPAm at 2:1 was performed at 4°C , well-defined nanospheres were formed as illustrated by both SEM and TEM images (a-b). By contrast, only drug crystals could be observed when the same mixture was dialyzed at 50°C (c-d).



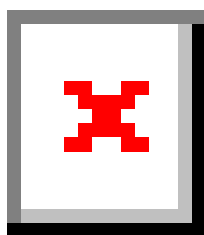
a



b

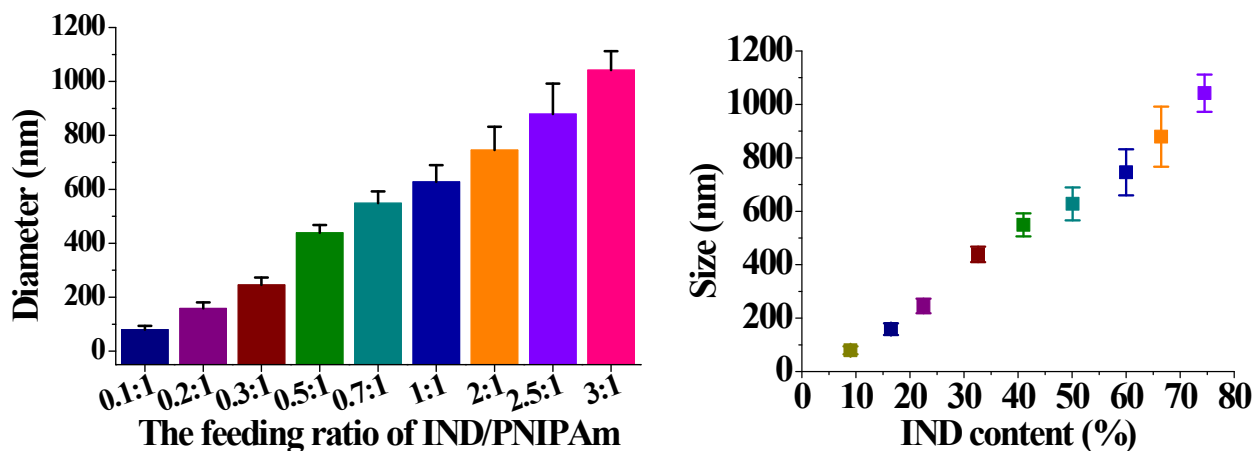


c

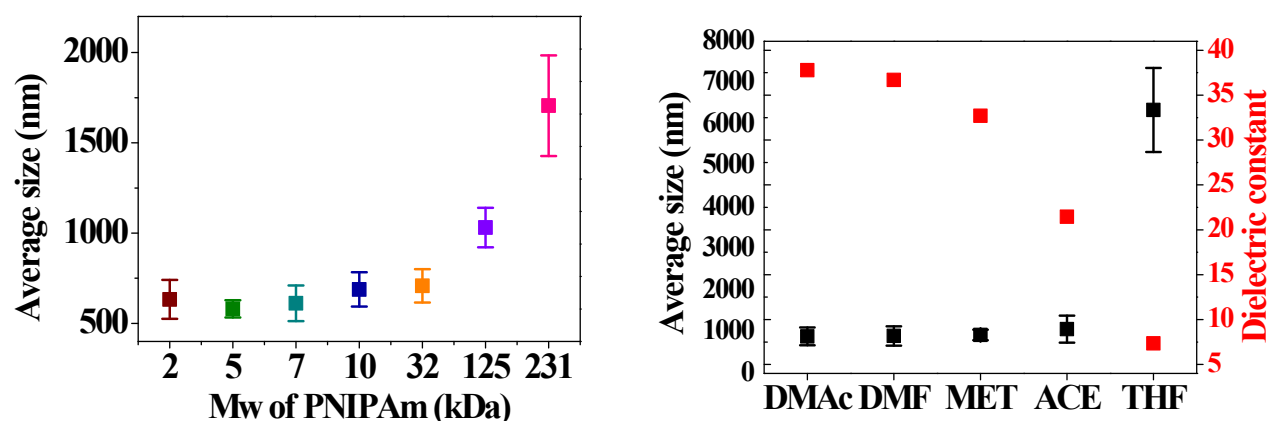


d

Fig. S6 Effects of H-bonding competitive additives on IND/PNIPAm assembly. **a-b**, SEM (a) and TEM (b) images of samples obtained in the presence of thiourea. **c-d**, SEM images of samples produced by dialysis with acetic acid (c) or propionic acid (d). IND/PNIPAm mixture at 2:1 in DMSO was dialyzed against deionized water containing 0.5 M thiourea, 1.4 M acetic acid, or 1.4 M propionic acid, respectively. First exchange of the outer water phase was carried out after 1 h, then it was refreshed every 2 h. After 12 h of dialysis, samples in dialysis tubing were collected for SEM or TEM observation.



a

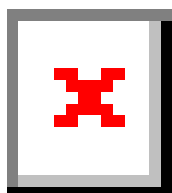


b

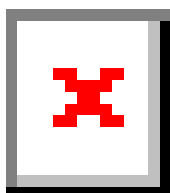
c

Fig. S7 Size of IND/PNIPAm assemblies fabricated under different conditions. **a**, The IND feeding effect. The x-axis of the left panel shows the theoretical IND/PNIPAm weight ratio, while the right one indicates the actual IND content in resultant assemblies. **b**, Effects of PNIPAm Mw. The IND/PNIPAm ratio was 2:1. **c**, Various common solvents. DMAc, dimethylacetamide; DMF, dimethylformamide; MET, methanol; ACE, acetone; and THF, tetrahydrofuran. To explore the effect of common solvents, the IND/PNIPAm ratio was kept at 1.5:1. PNIPAm with Mw of 10 kDa was used for studies on both drug loading and solvent effects.

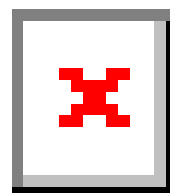
Note. Since dielectric constant (ϵ) of a solvent is a measure of its polarity, and water is a highly polar solvent ($\epsilon_{\text{water}} = 80$, which is notably higher than that of solvents employed), therefore a solvent with higher polarity may have stronger interactions with water. This facilitates molecular exchange between the organic phase and the water phase, thereby accelerating assembly into smaller particles.



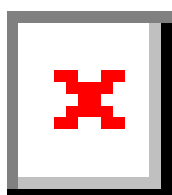
a



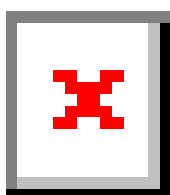
b



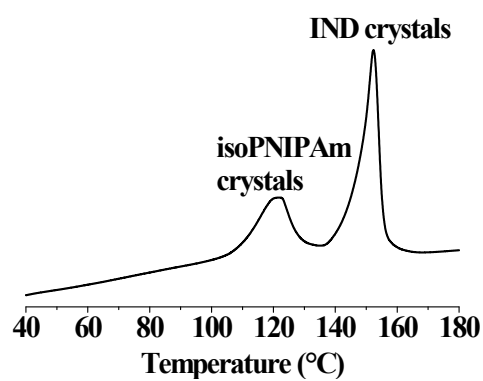
c



d



e



f

Fig. S8 SEM images of dialyzed IND/isoPNIPAm samples at various weight ratios. **a**, 0.5:1; **b**, 1:1; **c**, 1.5:1; **d**, 2:1; **e**, 3:1. **f**, The DSC curve of IND/isoPNIPAm aggregates at the drug/polymer weight ratio of 3:1.

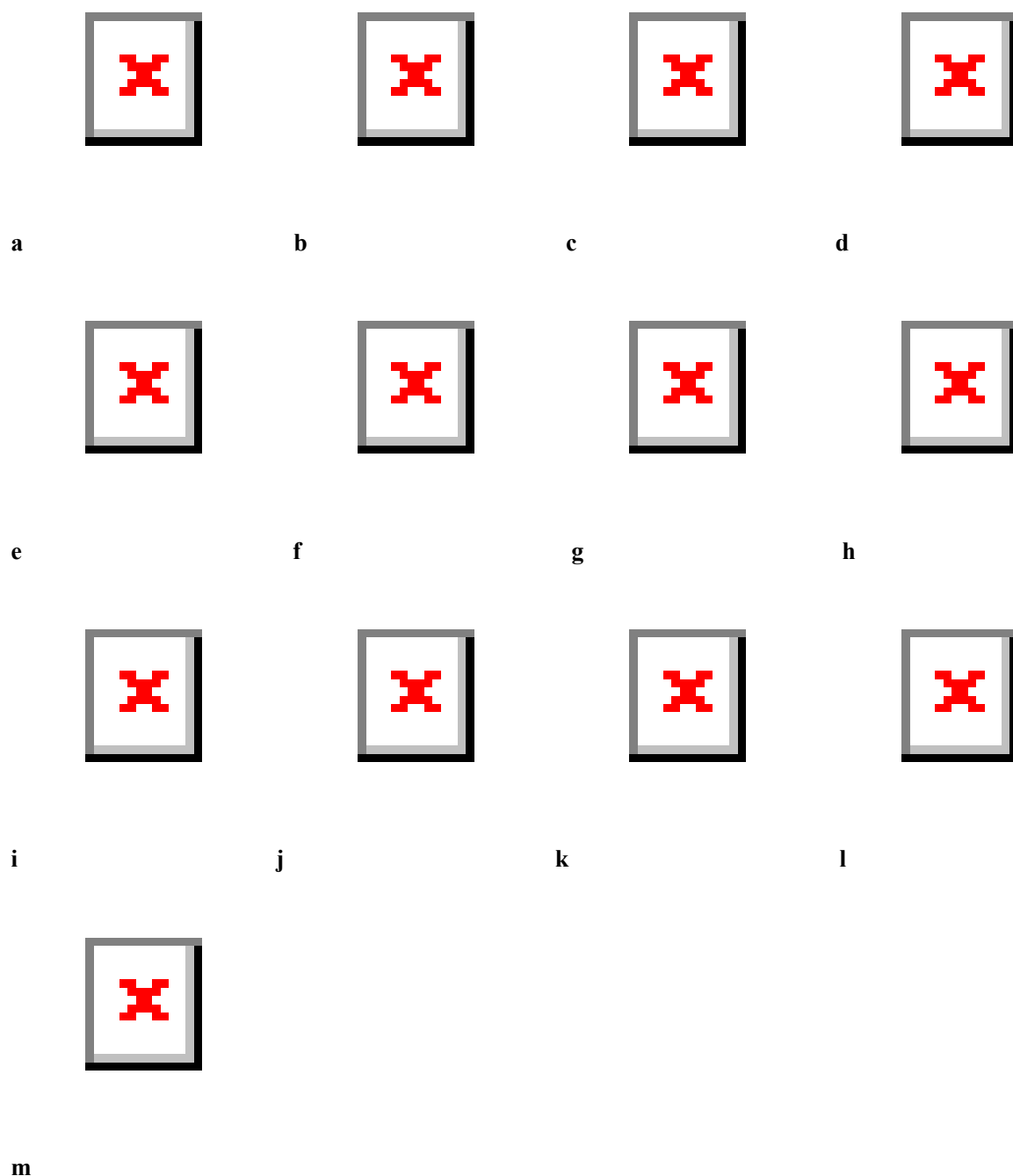
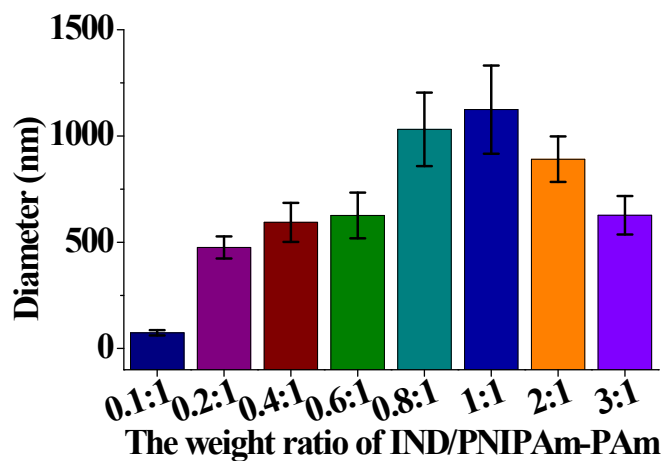
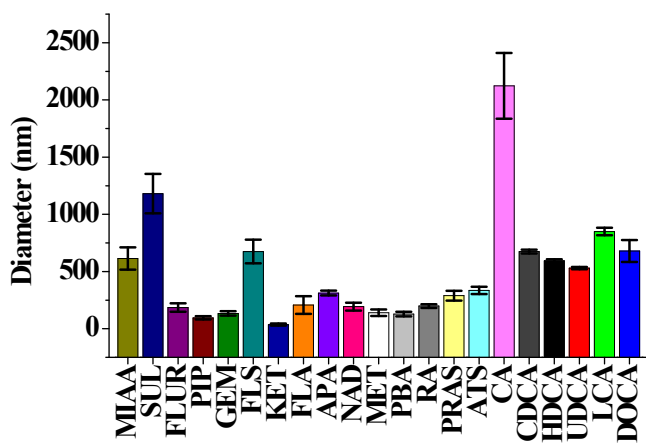
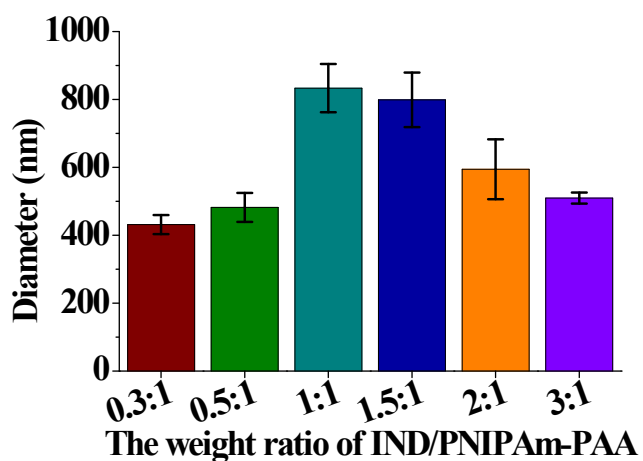


Fig. S9 Electron microscopy characterization of assemblies derived from PNIPAm and various biologically active CBCs. **a-i**, TEM images of nanoassemblies formed by PNIPAm and flufenamic acid (FLA) (a), *p*-acetamidophenyl acetic acid (APA) (b), ketoprofen (KET) (c), nadifloxacin (NAD) (d), methotrexate (MET) (e), 4-phenylbutyric acid (PBA) (f), retinoic acid (RA) (g), pravastatin (PRAS) (h), or atorvastatin (ATS) (i) at the CBC/PNIPAm weight ratio of 2:1. **j-m**, SEM images showing microspheres assembled by PNIPAm with cholic acid (CA) (j), lithocholic acid (LCA) (k), deoxycholic acid (DOCA) (l), and glycodeoxycholic acid (GDCA) (m). The CBC/PNIPAm weight ratio was 0.5:1 for GDCA, while it was 2:1 for CA, LCA, and DOCA.



a

b



c

Fig. S10 The average size of assemblies based on various CBC/polymer combinations. **a**, PNIPAm and various CBCs. **b**, IND/PNIPAm-PAm assemblies. **c**, IND/PNIPAm-PAA assemblies.



a **b**
Fig. S11 Electron microscopy images of PTX crystals after dialysis against deionized water. **a**, SEM; and **b**, TEM.

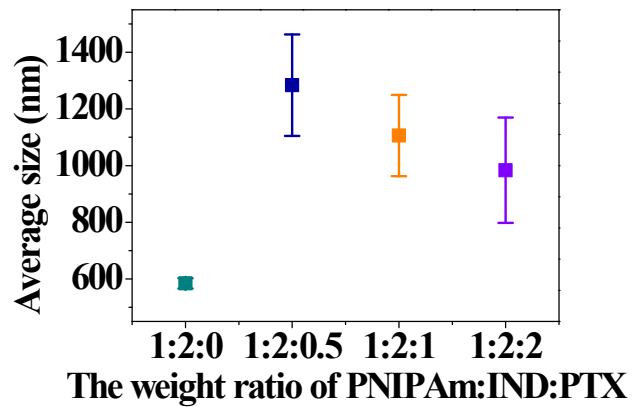


Fig. S12 The effect of PTX loading on the average size of assemblies containing PTX.

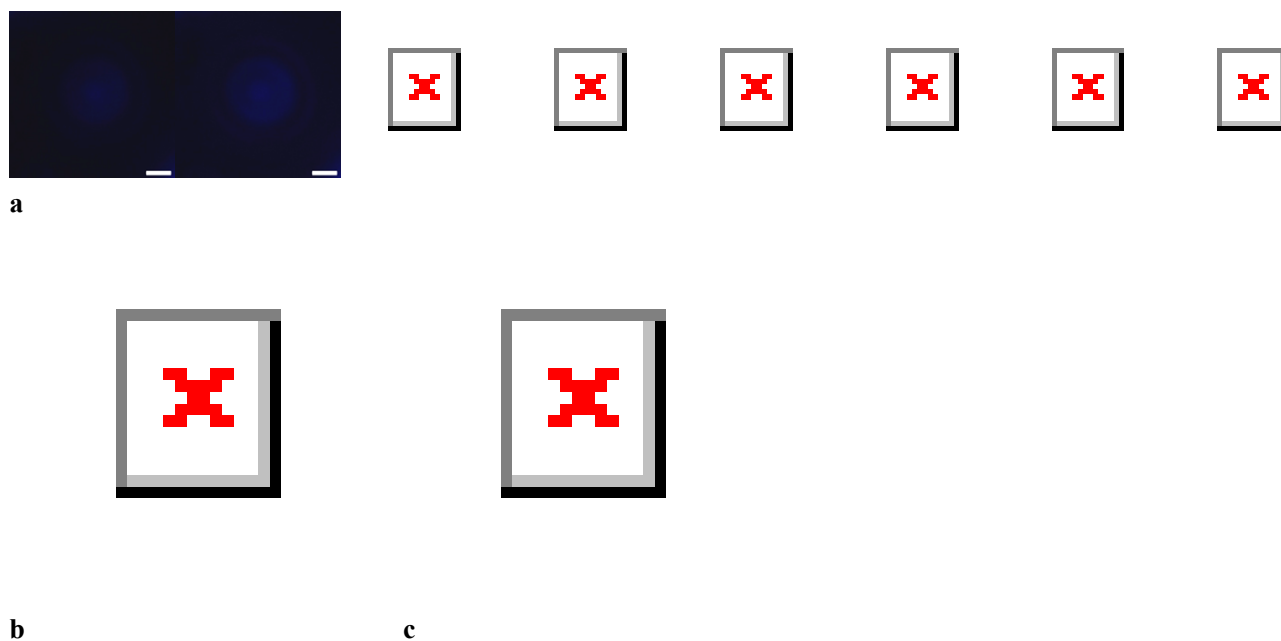


Fig. S13 CLSM images of various assemblies. **a**, Series images along z-axis showing multilayered structures of PNIPAm/IND/PTX assemblies at the weight ratio of 1:1:1. The scale bars represent 500 nm. **b-c**, Spherical assemblies based on PNIPAm/IND at the weight ratio of 1:2 (a) and 1:3 (b). The corresponding IND loading content was 66.% and 74.5% for the assemblies at 1:2 and 1:3, respectively.

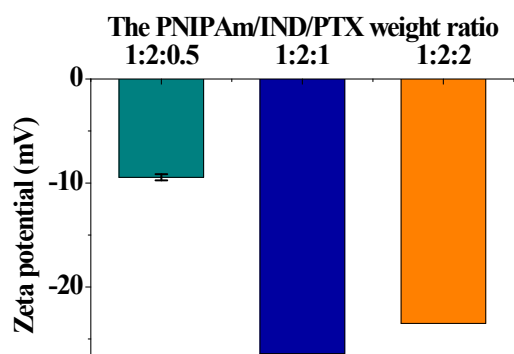


Fig. S14 Zeta potential values of PNIPAm/IND/PTX assemblies.